Imaging high-pressure rock exhumation in eastern Taiwan

D. Brown[1], Y.-M. Wu[2], K.-F. Feng[2], W.-A. Chao[2], and H.-H. Huang[3,4]
[1]Institute of Earth Science "Jaume Almera", CSIC, Barcelona E-08028, Spain
[2]Department of Geosciences, National Taiwan University, Taipei 106, Taiwan
[3]Department of Geology and Geophysics, University of Utah, Salt Lake City, Utah 84112, USA
[4]Division of Geological and Planetary Sciences, California Institute of Technology, Pasadena, California 91125, USA

ABSTRACT

Increasingly detailed studies of out crops of high-pressure rock terranes in combination with rapidly evolving numerical modeling studies have given rise to a number of possible explanations for the processes by which these rocks are exhumed. Imaging actively exhuming high-pressure terranes remains one of the fundamental, but elusive, tasks that could advance the understanding of how these important rocks reach Earth's surface. Seismic tomography along the active arc-continent collision in eastern Taiwan images a high P- and S-wave velocity zone that extends from the shallow subsurface beneath a high-pressure metamorphic terrane to ~50 km depth. We present a petrophysical analysis of this high-velocity zone that indicates the presence of rock types common to high-pressure terranes. The high-velocity zone is seismically active throughout. We determine focal mechanisms for 57 earthquakes, and carry out full waveform modeling on 10; these have double-couple focal mechanisms with a compensated linear vector dipole component up to 20.6%. We suggest that the high-velocity zone comprises an exhuming high-pressure terrane. Focal mechanisms for earthquakes within it indicate that shear faulting dominates in the deformation, but high fluid pressure may also play a role.

INTRODUCTION

Detailed studies of a large number of subduction-related high-pressure rock terranes, in combination with numerical modeling, indicate that various mechanisms may explain how these terranes are exhumed to Earth's surface (Erdman and Lee, 2014; Hacker and Gerya, 2013; Warren, 2013; Agard et al., 2009; Gerya et al., 2002). Despite noteworthy advances, there is still debate, and a significant number of unknowns, about the mechanisms of exhumation (Erdman and Lee, 2014; Warren, 2013; Hacker and Gerya, 2013). To help narrow the gap on these unknowns, important objectives for future research have been proposed, among which is the imaging of actively exhuming high-pressure terranes (Hacker and Gerya, 2013). A key question that arises from this suggestion is, how can a high-pressure rock terrane be recognized in a geophysical data set? Petrophysical analyses comparing in situ seismic wave velocities with those measured in the laboratory on a suite of rocks commonly found in high-pressure terranes can provide an answer. Compilations of the worldwide occurrences of high-pressure terranes show that they have many lithological characteristics in common (Maruyama et al., 1996; Ernst, 2005), thereby facilitating such a petrophysical study.

Quartz mica schist is by far the most abundant rock type making up high-pressure terranes (Ernst, 2005). Metamorphosed basalt from oceanic crust and volcanic arc-derived rocks are found in much smaller quantities, as are metabasic rocks such as amphibolite. Metamorphosed mantle-derived ultramafic rocks that are generally accompanied by serpentinite constitute only a small volume of many high-pressure terranes. In any one terrane, all or part of these rocks may have been metamorphosed under blueschist and/or eclogite facies conditions. Some high-pressure terranes form large, coherent units, while in others the high-pressure rocks are in smaller units as part of a tectonic mélange (a structural mixture of rock types of different metamorphic grades) (Kylander-Clark et al., 2013; Ernst, 2005).

HIGH-PRESSURE ROCKS IN EASTERN TAIWAN

Arc-continent collision has been taking place in Taiwan (Fig. 1) since the latest Miocene as the result of the subduction of the Eurasia plate beneath the Luzon arc on the Philippine Sea plate (Sibuet and Hsu, 2004). To the immediate west of the colliding volcanic arc, the fault-bounded Yuli belt (Fig. 1) forms a tectonic mélange that comprises predominantly greenschist facies quartz mica schist with isolated occurrences of metamorphosed oceanic crust, amphibolite, blueschist, and omphacite-zoisite metabasite with serpentinite (Keyser, 2015; Tsai et al., 2013; Sun et al., 1998; Yui and Lo, 1989; Liou, 1981). The age of peak metamorphism of the high-pressure rocks is not well constrained, but is thought to be between 5 and 14 Ma (e.g., Beyssac et al., 2008). Pressure and temperature estimates for the quartz-mica schist, the blueschist, and the omphacite-zoisite metabasite range from 0.6 to 1.7 GPa, and 400 to 550 °C (Keyser, 2015; Tsai et al., 2013; Beyssac et al., 2008). Apatite fission track ages in the Yuli belt range from ca. 0.9 to 0.4 Ma, suggesting exhumation rates of 3–12 mm yr^{-1} (Willett et al., 2003; Dadson et al., 2003), much higher than those of the metamorphic rocks to the west or the unmetamorphosed volcanic arc to the east.

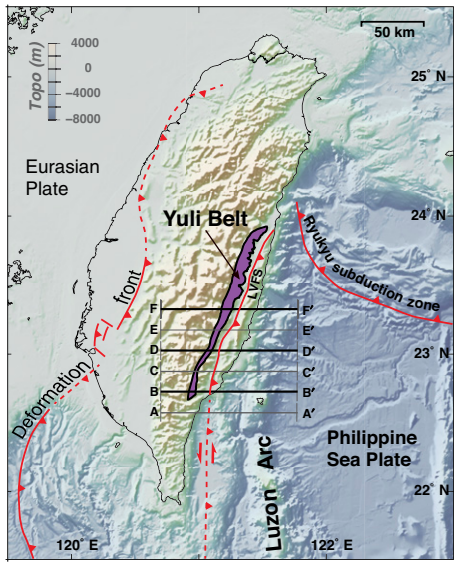

Figure 1. Digital elevation and bathymetry model of the Taiwan mountain belt and the surrounding ocean floor. The main tectonic boundaries are shown in red, and the high-pressure Yuli belt is in purple. Locations of the tomography sections shown in Figure 2 are indicated by thick black lines labeled B-B′, D-D′, and F-F′. Sections A-A′, C-C′, and E-E′ are shown in Figure DR1 (see footnote 1). LVFS—Longitudinal Valley fault system.

IMAGING HIGH-PRESSURE ROCKS

Seismic tomography across eastern Taiwan (Huang et al., 2014) images a zone of high P- and S-wave velocities (Vp and Vs, respectively) that dips eastward from below the Yuli belt and beneath the arc-continent suture (Longitudinal Valley fault system; LVFS in Fig. 2), to at least 50 km depth under the Luzon arc (Figs. 2A and 2B). South of the Yuli belt, the high-velocity zone forms a broad, open feature that narrows northward (Fig. 2; Fig. DR1 in the GSA Data Repository[1]). Vp and Vs range from ~7.8 and 4.4 km s^{-1} at 50 km depth to ~6.5 and 3.8 km s^{-1}

[1]GSA Data Repository item 2015229, methodologies, tomography sections not shown in the text, plots of velocities of all rock types investigated at each depth interval, Vp versus Vs and Vp versus Vp/Vs plots for the rocks of interest at 20 and 40 km depth, and focal mechanisms for the 57 events within the high-velocity zone and the wave form models for the 10 modeled events, is available online at www.geosociety.org/pubs/ft2015.htm, or on request from editing@geosociety.org or Documents Secretary, GSA, P.O. Box 9140, Boulder, CO 80301, USA.

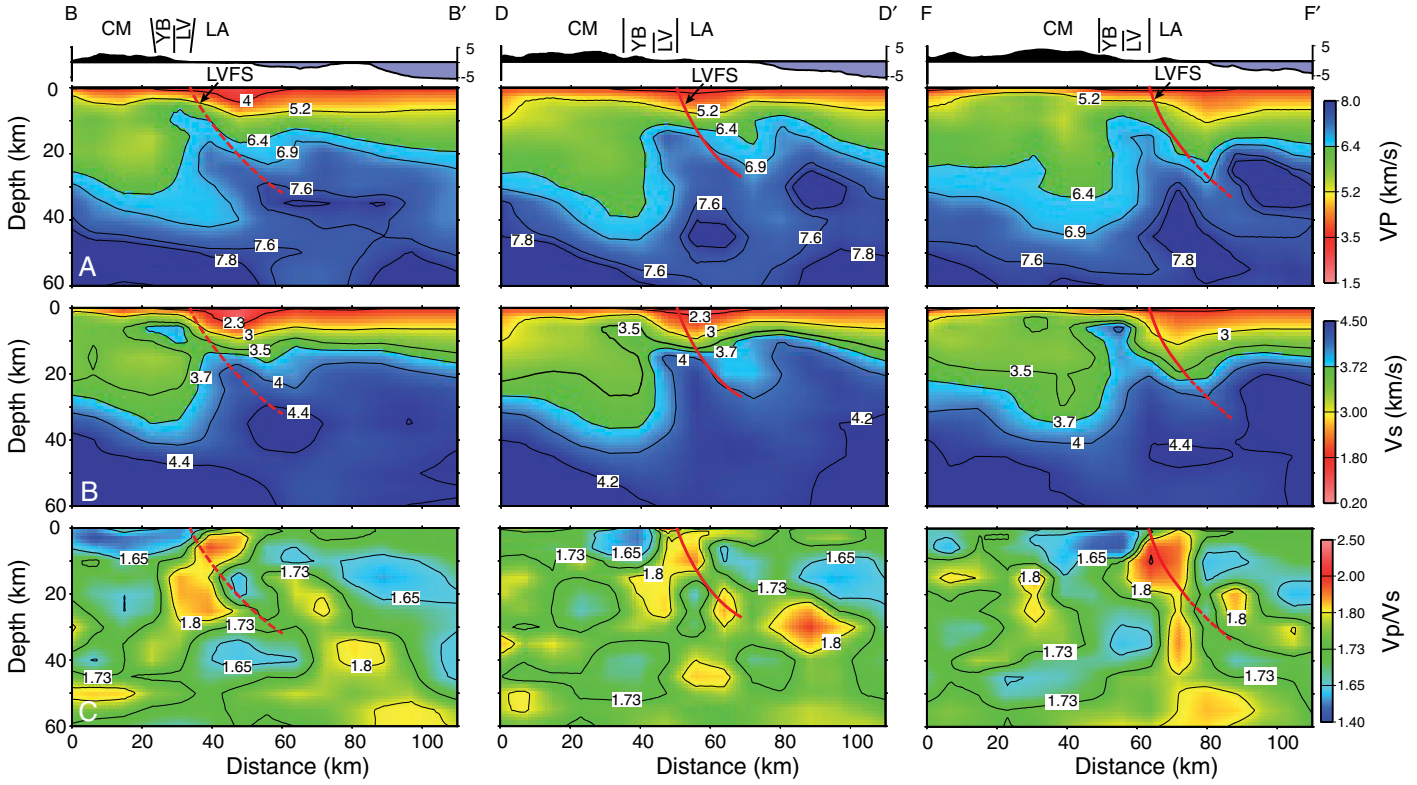

Figure 2. Tomographic velocity sections for eastern Taiwan (see text). A: P-wave. B: S-wave. C: Vp/Vs ratio. A zone of high P- and S-wave velocities extends from near the surface beneath the high-pressure Yuli belt (YB) and the Longitudinal Valley fault system (LVFS) to ~50 km depth. The high-velocity zone correlates with a high Vp/Vs ratio along much of its downdip extension. CM—continental margin; LA—Luzon arc; LV—Longitudinal Valley.

at 10 km depth. The Vp/Vs ratio is from 1.77 to 1.71 over the same depth range.

In order to determine the rock types that are present in the high-velocity zone, we compare the Vp, Vs, and Vp/Vs for a range of depths with measured seismic velocities from a large variety of rocks (Christensen, 1996). These were temperature corrected using a geothermal gradient of 10 °C km^{-1} (common for high-pressure rocks worldwide; e.g., Maruyama et al., 1996) and for effective pressure (for methods, see the Data Repository). Only those rocks that approximate the Vp, Vs, and the Vp/Vs ratios modeled in the tomography at the depth intervals of interest are discussed (Fig. 3; see Fig. DR2). At 10 km depth, several metamorphosed continental and volcanic arc rock types fit well with the in situ velocities. Mantle rock types have a poor fit at this depth. By 20 km depth (Fig. DR3), most continental rock types have moved out of the field of the in situ velocity, whereas metamorphosed arc rock types, hornblendite, and blueschist (including those in the Yuli belt) enter it. Mantle rock types with 20%–30% serpentinization begin to approach the Vp and Vs range, but with this serpentine content their Vp/Vs ratios would be high. By 30 km depth, arc rock types have moved out of the field of interest, which is now occupied by blueschist, pyroxenite, harzburgite, lherzolite, and dunite with 10%–20% serpentinization. At 40 and 50 km depth (Fig. 3), eclogite, pyroxenite, and weakly to unserpentinized harzburgite, lherzolite, and dunite best fit the Vp, Vs, and Vp/Vs range of interest.

SEISMICITY WITHIN THE HIGH-PRESSURE TERRANE

A corollary to our imaging a high-pressure terrane is that it is seismically active throughout. Earthquakes within the high-pressure terrane extend from the surface to ~50 km depth, deeper than the seismicity cluster defining the arc-continent suture (LVFS in Fig. 4). Earthquake magnitudes are as high as M_L 5.1. From the large number of earthquakes, focal mechanisms were determined for 57 events between M_L 3.4 and 5.1 (Fig. DR4; for methods, see the Data Repository). While there is no clear pattern to their distribution, events have predominately oblique-slip and thrust focal mechanisms between 10 km and 30 km depth, whereas strike-slip, oblique-slip, and extensional focal mechanisms dominate between 30 km and 50 km depth. The majority of extensional events occur near the base of the seismicity. We chose 10 high-quality events for full waveform modeling of their stress tensors. These were decomposed into double-couple and compensated linear vector dipoles (CLVD) (Fig. 4; Fig. DR4). These 10 events have predominately double-couple focal mechanisms, the CLVD component ranging from 0.5% to 20.6%.

DISCUSSION AND CONCLUSIONS

The petrophysical analysis indicates that the high-velocity zone imaged in the seismic tomography can be matched to rock types found in high-pressure terranes, making this the first time that an actively exhuming terrane has been clearly imaged. The surface area of the Yuli belt (~1700 km^2), combined with the depth extension and thickness of the high-velocity zone, makes it a large type (Kylander-Clark et al., 2013) high-pressure terrane. The mechanism of exhumation appears to be subduction channel flow (Hacker and Gerya, 2013; Warren, 2013; Gerya et al., 2002). In this scenario, material from the subducting continental crust, the overriding volcanic arc, and the upper plate mantle are being forced upward against a steep buttress of lower velocity material while being overthrust by the volcanic arc. The petrophysical data indicate a change in the lithological composition of the terrane from the mélange of mostly pelitic metasediments with lesser oceanic and volcanic arc crustal rock types at the surface and in the upper 20 km to 30 km, to predominantly mantle rock types and eclogite at greater depth. Such lithological stratification has also been noted in numerical models of high-pressure ter-

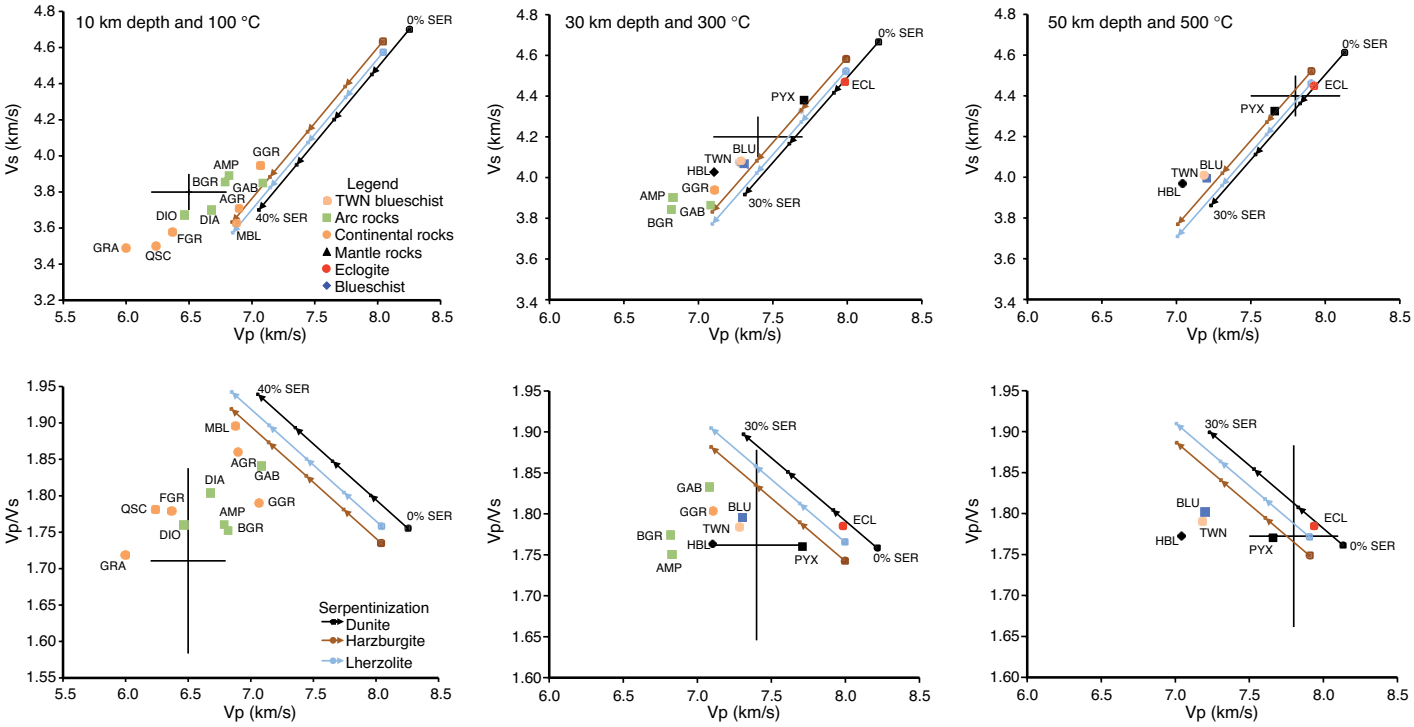

Figure 3. Vs versus Vp, and Vp/Vs versus Vp (see text); black cross indicates plots for rock types near the range of interest. The maximum velocity is determined from the tomography data at each depth interval and the range is set so as not to cross the low-velocity zone to the west and the Longitudinal Valley fault system (LVFS) to the east. The lateral range at each depth interval of Vp is 0.3 km s^{-1}, and Vs is 0.1 km s^{-1}. The Vp/Vs range is calculated from these. For plots at 20, 40, and 50 km depth see Figure DR3 (see footnote 1). The labels (i.e., BZE) are explained in Figure DR2. The lines for DUN, HRZ, and LHZ represent the change in Vp, Vs, and Vp/Vs with degree of serpentinization.

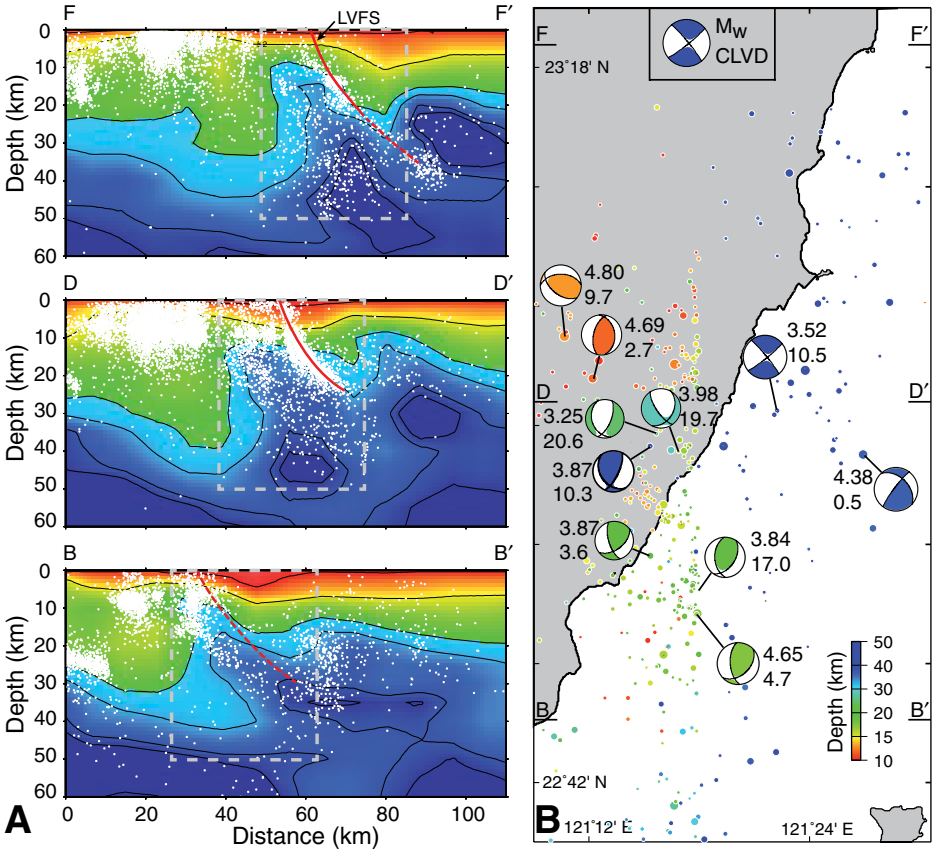

Figure 4. Seismicity data within the study area and focal mechanism data from the high-velocity zone (see text). A: P-wave tomography sections with earthquakes projected on to them from 9.99 km on each side. The gray box indicates the part of the section shown in B. Velocity scale as in Figure 2. Red line is Longitudinal Valley fault system (LVFS). B: Full waveform modeling of focal mechanisms was carried out for 10 high-quality events. These were decomposed into double-couple and compensated linear vector dipoles (CLVD) components (see inset; M_w—moment magnitude). The waveform analyses are given in Figure DR4 (see footnote 1).

rane formation where they are thought to result from density and rheological differences (Gerya and Stöckhert, 2006). Our data further suggest that at deeper levels in the subduction channel arc lower crust and eventually mantle rock types dominate as they are incorporated from the upper plate. The Vp/Vs data suggest that serpentinized lherzolite, harzburgite, and dunite are not present in large volumes in the upper 30 km, whereas below this they may contain as much as 20% serpentine. We stress, however, that with petrophysical data it is impossible to determine the volume proportions of each rock type at any one point.

The petrophysical analysis indicates the presence within the high-pressure terrane of metamorphic rock types that are rich in hydrous minerals such as mica, chlorite, amphibole, and especially serpentine. Dewatering of these could cause dehydration embrittlement of the rock and a resultant rise in fluid pressure that might be sufficient to cause seismic rupturing (e.g., Hacker et al., 2003; Dobson et al., 2002; Green and Houston, 1995). Fluid overpressuring can cause tensile fracturing that produces earthquakes, and these earthquakes could have a significant non–double-couple component (Frohlich, 1989; Julian et al., 1998). Our seismicity data contain only three events with a sufficient CLVD component (~20%) that they can be reliably interpreted as a deviation from a pure double-couple focal mechanism. Nevertheless, the seismicity data indicate that the high-pressure terrane is deforming internally by complex faulting mechanisms. Shear faulting with double-couple focal mechanisms is dominant, although in three events a moderate CLVD component suggests that dehydration embrittlement and fluid overpressuring may also play important roles in the deformation and exhumation processes of this high-pressure terrane.

ACKNOWLEDGMENTS

Funding was provided by MICINN grant CGL2013-43877-P and MOST grant 103-2811-M-002-053. We thank B. Hacker, T. Gerya, and two anonymous reviewers for their comments.

REFERENCES CITED

Agard, P., Yamato, P., Jolivert, L., and Burov, E., 2009, Exhumation of oceanic blueschists and eclogites in subduction zones: Timing and mechanisms: Earth-Science Reviews, v. 92, p. 53–79, doi:10.1016/j.earscirev.2008.11.002.

Beyssac, O., Negro, F., Simoes, M., Chan, Y.-C., and Chen, Y.-G., 2008, High-pressure metamorphism in Taiwan: From oceanic subduction to arc-continent collision?: Terra Nova, v. 20, p. 118–125, doi:10.1111/j.1365-3121.2008.00796.x.

Christensen, N.I., 1996, Poisson's ratio and crustal seismology: Journal of Geophysical Research, v. 101, p. 3139–3156, doi:10.1029/95JB03446.

Dadson, S.J., et al., 2003, Links between erosion, runoff variability and seismicity in the Taiwan orogen: Nature, v. 426, p. 648–651, doi:10.1038/nature02150.

Dobson, P., Meredith, P.G., and Boon, S.A., 2002, Simulation of subduction zone seismicity by dehydration of serpentine: Science, v. 298, p. 1407–1410, doi:10.1126/science.1075390.

Erdman, M.E., and Lee, C.-Y.A., 2014, Oceanic- and continental-type metamorphic terranes: Occurrence and exhumation mechanisms: Earth-Science Reviews, v. 139, p. 33–46, doi:10.1016/j.earscirev.2014.08.012.

Ernst, W.G., 2005, Alpine and Pacific styles of Phanerozoic mountain building: Subduction-zone petrogenesis of continental crust: Terra Nova, v. 17, p. 165–188, doi:10.1111/j.1365-3121.2005.00604.x.

Frohlich, C., 1989, The nature of deep-focus earthquakes: Annual Review of Earth and Planetary Sciences, v. 17, p. 227–254, doi:10.1146/annurev.ea.17.050189.001303.

Gerya, T., and Stöckhert, B., 2006, Two-dimensional numerical modeling of tectonic and metamorphic histories at active continental margins: International Journal of Earth Sciences, v. 95, p. 250–274, doi:10.1007/s00531-005-0035-9.

Gerya, T.V., Stöckhert, B., and Perchuk, A.L., 2002, Exhumation of high-pressure metamorphic rocks in a subduction channel: A numerical simulation: Tectonics, v. 21, 1056, doi:10.1029/2002TC001406.

Green, H.W., and Houston, H., 1995, The mechanics of deep earthquakes: Annual Review of Earth and Planetary Sciences, v. 23, p. 169–213, doi:10.1146/annurev.ea.23.050195.001125.

Hacker, B.R., and Gerya, T.V., 2013, Paradigms, new and old, for ultrahigh-pressure tectonism: Tectonophysics, v. 603, p. 79–88, doi:10.1016/j.tecto.2013.05.026.

Hacker, B.R., Peacock, S.M., Abers, G.A., and Holloway, S.D., 2003, Subduction factory 2. Are intermediate-depth earthquakes in subducting slabs linked to metamorphic dehydration reactions?: Journal of Geophysical Research, v. 108, *2030,* doi:10.1029/2001JB001129.

Huang, H.-H., Wu, Y.-M., Song, X., Chang, C.-H., Lee, S.-J., Chang, T.-M., and Hsieh, H.-H., 2014, Joint Vp and Vs tomography of Taiwan: Implications for subduction-collision orogeny: Earth and Planetary Science Letters, v. 392, p. 177–191, doi:10.1016/j.epsl.2014.02.026.

Julian, B.R., Miller, A.D., and Foulger, G.R., 1998, Non-double-couple earthquakes 1. Theory: Reviews of Geophysics, v. 36, p. 525–549, doi:10.1029/98RG00716.

Keyser, W.M., 2015, Petrology and equilibrium phase modeling of metamorphic rocks from the Chinshuichi area of the Yuli Belt in eastern Taiwan [M.S. thesis]: Hualien, Taiwan, National Dong Hwa University, 166 p.

Kylander-Clark, A.R.C., Hacker, B.R., and Mattinson, C.G., 2013, Size and exhumation rate of ultrahigh-pressure terranes linked to orogenic stage: Earth and Planetary Science Letters, v. 321–322, p. 115–120, doi:10.1016/j.epsl.2011.12.036.

Liou, J.G., 1981, Petrology of metamorphosed oceanic rocks in the Central Range of Taiwan: Geological Society of China Memoir 4, p. 291–341.

Maruyama, S., Liou, J.G., and Terabayashi, M., 1996, Blueschists and eclogites of the world and their exhumation: International Geology Review, v. 38, p. 485–594, doi:10.1080/00206819709465347.

Sibuet, J.-C., and Hsu, S.-K., 2004, How was Taiwan created?: Tectonophysics, v. 379, p. 159–181, doi:10.1016/j.tecto.2003.10.022.

Sun, C.-H., Smith, A.D., and Chen, C.-H., 1998, Nd-Sr isotopic and geochemical evidence on the protoliths of exotic blocks in the Juisui area, Yuli Belt, Taiwan: International Geology Review, v. 40, p. 1076–1087, doi:10.1080/00206819809465255.

Tsai, C.-H., Iizuka, Y., and Ernst, W.G., 2013, Diverse mineral compositions, textures, and metamorphic P-T conditions of the glaucophane-bearing rocks in the Tamayen melange, Yuli Belt, eastern Taiwan: Journal of Asian Earth Sciences, v. 63, p. 218–233, doi:10.1016/j.jseaes.2012.09.019.

Warren, C.J., 2013, Exhumation of (ultra-) high-pressure terranes: Concepts and mechanisms: Solid Earth, v. 4, p. 75–92, doi:10.5194/se-4-75-2013.

Willett, S.D., Fisher, D., Fuller, C., Yeh, E.-C., and Lu, C.-Y., 2003, Erosion rates and orogenic-wedge kinematics in Taiwan inferred from fission-track thermochronometry: Geology, v. 31, p. 945–948, doi:10.1130/G19702.1.

Yui, T.-F., and Lo, C.-H., 1989, High-pressure metamorphosed ophiolitic rocks from the Wanjung area, Taiwan: Geological Society of China Proceedings, v. 32, p. 47–62.

Manuscript received 21 March 2015
Revised manuscript received 19 May 2015
Manuscript accepted 22 May 2015

Printed in USA